Available online at www.sciencedirect.com
ScienceDirect
Journal of the European Ceramic Society 28 (2008) 1657–1663
www.elsevier.com/locate/jeurceramsoc

Growth behaviour of potassium sodium niobate single crystals grown by solid-state crystal growth using $K_4CuNb_8O_{23}$ as a sintering aid

John G. Fisher [1], Andreja Benčan *, Jerneja Godnjavec, Marija Kosec

Department of Electronic Ceramics, Jožef Stefan Institute, Jamova 39, Ljubljana 1000, Slovenia

Received 28 June 2007; received in revised form 12 November 2007; accepted 25 November 2007
Available online 4 February 2008

Abstract

The effect of addition of 0, 0.5 and 2 mol% $K_4CuNb_8O_{23}$ liquid phase sintering aid on the growth of single crystals of $(K_{0.5}Na_{0.5})NbO_3$ by solid-state crystal growth (SSCG) was studied. Single crystal growth in the samples with 0 and 0.5 mol% $K_4CuNb_8O_{23}$ was initially rapid and then tailed off with annealing time, due to matrix grain growth which reduced the driving force for crystal growth. Addition of 0.5 mol% $K_4CuNb_8O_{23}$ caused a reduction in both single crystal and matrix grain growth rates. Addition of 2 mol% $K_4CuNb_8O_{23}$ caused matrix grain growth to stagnate, resulting in an almost constant driving force and constant crystal growth during annealing. Single crystals grown using 0 and 0.5 mol% $K_4CuNb_8O_{23}$ were stoichiometric, but single crystals grown with 2 mol% $K_4CuNb_8O_{23}$ were Na-rich. This was due to lowering of the solidus temperature by addition of $K_4CuNb_8O_{23}$.

Keywords: Single crystals; Grain growth; Interfaces; Niobates; Perovskites; (K, Na)NbO_3

1. Introduction

Due to the toxic nature of lead, there is a great interest in the development of lead-free piezoelectric ceramics. The mixed niobate system $(K_{1-x}Na_x)NbO_3$ and its derivatives are promising candidates for lead-free piezoelectric ceramics. The $(K_{1-x}Na_x)NbO_3$ system has a morphotropic phase boundary close to the $(K_{0.5}Na_{0.5})NbO_3$ composition, and ceramics of this composition display optimum piezoelectric properties in the system.[1,2] $(K_{0.5}Na_{0.5})NbO_3$ has moderate piezoelectrical properties[1–3] which can be improved by substitution with Li and Ta.[4,5]

Single crystals of several lead-free systems have excellent piezoelectric properties, especially when combined with crystallographic engineering.[6,7] It is expected that single crystals of $(K_{0.5}Na_{0.5})NbO_3$ would also have good piezoelectric properties. Single crystals of $(K_{1-x}Na_x)NbO_3$ have been grown by the flux method.[8–11] Difficulties were experienced by several workers in growing crystals with high K contents, but recently crystals with a composition of $(K_{0.47}Na_{0.53})NbO_3$ were grown using a KF/NaF flux.[11]

Single crystals of $(K_{0.5}Na_{0.5})NbO_3$ and Li/Ta-substituted $(K_{0.5}Na_{0.5})NbO_3$ have recently been grown by the solid-state crystal growth method.[12,13] In this method, a single crystal (called a seed crystal) is buried and then compacted in a ceramic powder. The sample is sintered and a single crystal of the ceramic composition grows epitaxially on the seed crystal. When the $(K_{0.5}Na_{0.5})NbO_3$ and Li/Ta-substituted $(K_{0.5}Na_{0.5})NbO_3$ single crystals were grown, $K_4CuNb_8O_{23}$ was added as a liquid phase sintering aid.[12,13] For single crystals of PMN-PT grown by SSCG, addition of up to a certain amount of PbO as a liquid phase sintering aid was found to promote single crystal growth, with further additions retarding crystal growth or having no effect.[14,15] It is expected that changing the amount of liquid phase sintering aid will also affect single crystal growth of $(K_{0.5}Na_{0.5})NbO_3$, but this has not yet been studied. In the present work, single crystals of $(K_{0.5}Na_{0.5})NbO_3$ have been grown using different amounts of $K_4CuNb_8O_{23}$ liquid phase sintering aid. The effect of sintering aid upon single crystal growth rate, grain growth in the matrix and chemical composition of the single crystal and the matrix grains has been investigated.

* Corresponding author. Tel.: +386 1 477 3256; fax: +386 1 477 3887.
E-mail address: andreja.bencan@ijs.si (A. Benčan).
[1] Current address: Department of Materials Science and Engineering, Korea Advanced Institute of Science and Technology, 373-1 Kusong-Dong, Yusong-gu, Daejon 305-701, Republic of Korea.

0955-2219/$ – see front matter © 2008 Elsevier Ltd. All rights reserved.
doi:10.1016/j.jeurceramsoc.2007.11.010

2. Experimental

Powders of $(K_{0.5}Na_{0.5})NbO_3$ and $K_4CuNb_8O_{23}$ were prepared using the methods in Ref. 12. Both powders were examined by X-ray diffraction and found to be single phase. Different amounts of $K_4CuNb_8O_{23}$ were added to the $(K_{0.5}Na_{0.5})NbO_3$ powder, followed by planetary milling in acetone with ZrO_2 media for 1 h. Powders were made with additions of 0, 0.5 and 2 mol% $K_4CuNb_8O_{23}$.

$KTaO_3$ single crystals (FEE GmbH, Germany) oriented in the ⟨0 0 1⟩ direction were used as seed crystals. The ⟨0 0 1⟩ direction was used because crystals grown in this direction have planar growth fronts, making measurement of growth distance possible.[12] The single crystals were supplied as plates of dimensions 5 mm × 5 mm × 1 mm, with one face of each crystal polished to a 0.25 μm finish. Seed crystals were prepared by cutting each plate into quarters with a diamond wire saw, followed by ultrasonic cleaning in acetone. To make the samples, seed crystals of dimensions approximately 2 mm × 2 mm × 1 mm were again ultrasonically cleaned in acetone and then buried in 1 g of powder in an 8 mm diameter die. Samples were uniaxially pressed at 60 MPa, followed by cold isostatic pressing at 200 MPa. The samples were then hot pressed in air at 975 °C and 50 MPa for 2 h. Heating and cooling rates were 5 °C min^{-1}. Hot pressed samples were vertically sectioned into two halves using a diamond wire saw and ultrasonically cleaned in acetone.

To reduce alkali volatilization, for each crystal growth experiment, half of a hot pressed sample was wrapped in Pt foil and buried in packing powder in an alumina crucible with a lid. The packing powder was of the same composition as the sample. The crucible was then placed in another crucible with a lid and placed in a tube furnace which could sinter samples under vacuum or under a controlled atmosphere. Samples were annealed at 1100 °C for between 1 and 20 h. All heating and cooling rates were 5 °C min^{-1}. During heating from room temperature to 400 °C, the samples were degassed under vacuum to remove adsorbed water. All further heating, annealing and cooling steps were then carried out under flowing synthetic air which had been passed through a desiccating column filled with silica gel. The weight of each sample was measured before and after each crystal growth experiment. In all cases, weight loss was ≤0.5%. Separate Pt foils and crucibles were used for the samples without and with $K_4CuNb_8O_{23}$.

Samples were polished to a 0.25 μm finish and characterized using a scanning electron microscope (SEM, JEOL 5800, Tokyo, Japan) equipped with a LINK ISIS 300 energy-dispersive X-ray spectrometer (EDS). For microstructural characterization, samples were thermally etched at 1050 °C for 1 h and carbon coated. Single crystal growth distance was measured from SEM micrographs. For each single crystal, 100 measurements of the growth distance were made and the mean growth distance calculated. Errors may be introduced into the measurement of the single crystal growth distance because the plane of polish may not be parallel to the [0 0 1] growth direction of the single crystal. To compensate for these errors, the thickness of each seed crystal was measured with a micrometer before it was buried in the powder. The thickness of the seed crystal was then measured again after the crystal growth experiments from optical micrographs (Nikon Eclipse TS100). By determining the ratio of the seed thickness as measured by micrometer to the seed thickness measured from the micrographs, the true single crystal growth distance could be calculated. The mean equivalent spherical 2D matrix grain radius was calculated from SEM micrographs using image analysis software (UTHSCSA Image Tool, The University of Texas Health Science Centre in San Antonio, USA). For each sample, at least 300 matrix grains were analyzed.

For chemical analysis, samples were polished but not etched. Samples were carbon coated. Single crystals of $KNbO_3$ and $NaNbO_3$ were used as standards.[16,17] The samples were analyzed using an accelerating voltage of 20 keV, a spectrum acquisition time of 60 s, a 35° take off angle and a 0° specimen tilt.

3. Results

Fig. 1(a)–(c) shows SEM secondary electron images of polished and etched samples that had been annealed at 1100 °C for 10 h. In the sample with 0 mol% $K_4CuNb_8O_{23}$, a single crystal layer up to 200 μm thick has grown on the seed crystal (Fig. 1(a)). The boundary between the single crystal and the matrix grains is not regular, but varies by as much as 60 μm. In the sample with 0.5 mol% $K_4CuNb_8O_{23}$, the growth distance of the single crystal has been reduced to 110 μm and the boundary between the single crystal and the matrix is now regular (Fig. 1(b)). In the sample with 2 mol% $K_4CuNb_8O_{23}$, the growth distance of the single crystal increases to 225 μm and the boundary between the single crystal and the matrix remains regular (Fig. 1(c)). Fig. 1(d) is an SEM backscattered electron image of a polished sample with 2 mol% $K_4CuNb_8O_{23}$ after annealing for 10 h. A secondary phase is present inside the single crystal and between the matrix grains. EDS of this phase showed it to contain Na, K, Cu and Nb. This phase is the $K_4CuNb_8O_{23}$ sintering aid. The Na present in this phase comes from dissolved $(K_{0.5}Na_{0.5})NbO_3$.[12] In the samples with 0.5 mol% $K_4CuNb_8O_{23}$ this phase was present in the matrix but not in the single crystal. No secondary phases were visible in the samples with 0 mol% $K_4CuNb_8O_{23}$.

Fig. 2 shows SEM secondary electron images of the matrix grains from the samples in Fig. 1. Fig. 2(a) shows the matrix of the sample with 0 mol% $K_4CuNb_8O_{23}$. The matrix grains are coarse, with a wide grain size distribution. The grain boundaries appear faceted. Porosity is visible at the grain triple junctions. When 0.5 mol% $K_4CuNb_8O_{23}$ is added, the matrix grain size is reduced and the shape of the grains also becomes more faceted with rounded corners (Fig. 2(b)). Pores are trapped inside some of the larger grains. When 2 mol% of $K_4CuNb_8O_{23}$ is added, the matrix grain size is reduced still further (Fig. 2(c)). The matrix grain shape remains faceted with round corners.

Fig. 3 shows measurements of the growth distance of the single crystals versus annealing time. The values at an annealing time of 0 h are the growth distances of the as-hot-pressed samples before any subsequent annealing took place. The data points are the mean growth distance, and the error bars are the standard deviation of the growth distance. The error bars give an indi-

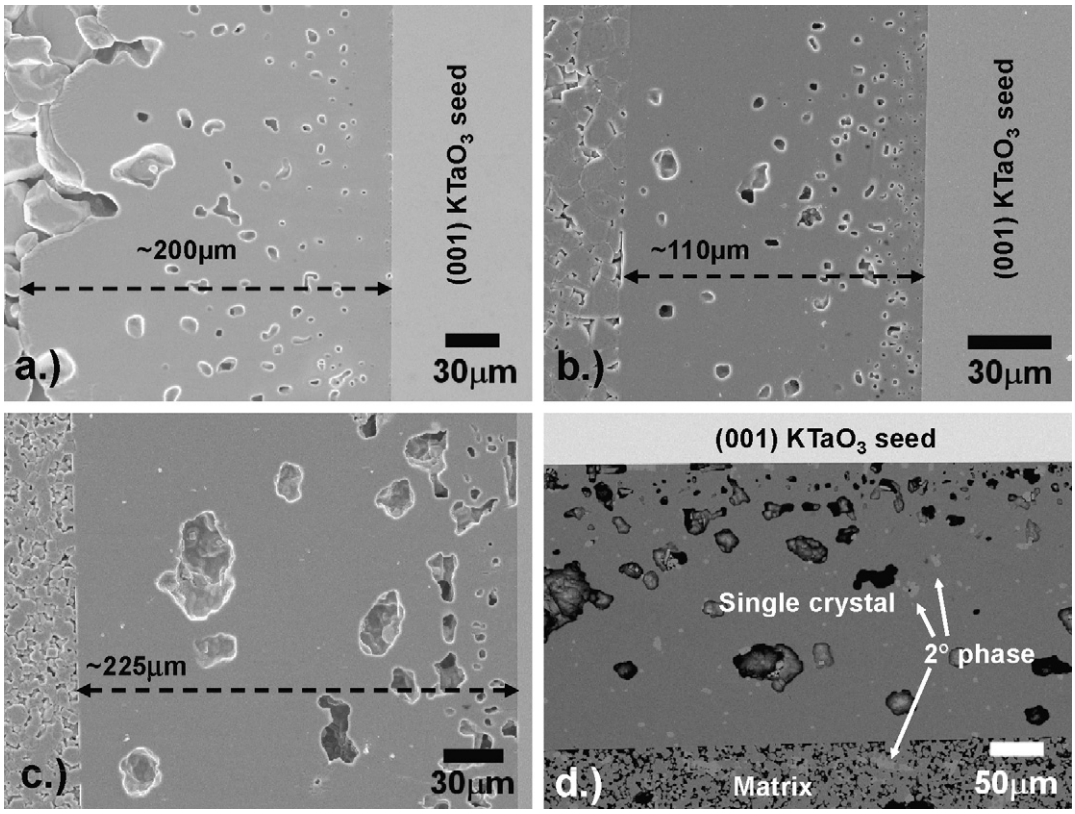

Fig. 1. SEM secondary electron images of single crystals grown in samples with (a) 0 mol%, (b) 0.5 mol% and (c) 2 mol% $K_4CuNb_8O_{23}$ after annealing at 1100 °C for 10 h. (d) SEM backscattered electron image of single crystal grown in sample with 2 mol% $K_4CuNb_8O_{23}$ after annealing at 1100 °C for 10 h.

cation of how regular the single crystal/matrix boundary is. In the samples with 0 mol% $K_4CuNb_8O_{23}$, single crystal growth is initially rapid but tails off as the annealing time increases above 5 h. The single crystal/matrix boundary is initially regular, but becomes increasingly irregular as annealing time increases. In the samples with 0.5 mol% $K_4CuNb_8O_{23}$, the growth distance is reduced compared to the samples with 0 mol% $K_4CuNb_8O_{23}$. Again, crystal growth is initially rapid but falls off with increasing annealing time. The crystal growth rate becomes almost constant after 5 h. The single crystal/matrix boundary remains regular even at extended annealing times. When 2 mol% of $K_4CuNb_8O_{23}$ is added, single crystal growth is rapid up to 1 h, but then tails off and becomes almost constant after 3 h. For annealing times up to 5 h, the growth distance of the single crystals in samples with 2 mol% $K_4CuNb_8O_{23}$ are similar to those in the samples with 0.5 mol% $K_4CuNb_8O_{23}$. However, the crystals in samples with 2 mol% $K_4CuNb_8O_{23}$ keep on growing at the same rate after 5 h, whereas crystal growth in the samples with 0 and 0.5 mol% $K_4CuNb_8O_{23}$ slows down. By 10 h the single crystal growth distance of the samples with 2 mol% $K_4CuNb_8O_{23}$ has become greater than that of the samples with 0 mol% $K_4CuNb_8O_{23}$. The single crystal growth rate of the samples with 2 mol% $K_4CuNb_8O_{23}$ drops slightly after 10 h.

The change in the matrix grain size with annealing time is shown in Fig. 4. The mean equivalent spherical 2D grain radius is plotted. The values at an annealing time of 0 h are the mean grain radii of the as-hot-pressed samples before any subsequent annealing took place. In the samples with 0 mol% $K_4CuNb_8O_{23}$, the matrix grains grow up to an annealing time of 10 h, at which point grain growth ceases at a mean grain radius of 7 μm. In the samples with 0.5 mol% $K_4CuNb_8O_{23}$, the matrix grain size is smaller than that of the samples with 0 mol% $K_4CuNb_8O_{23}$.

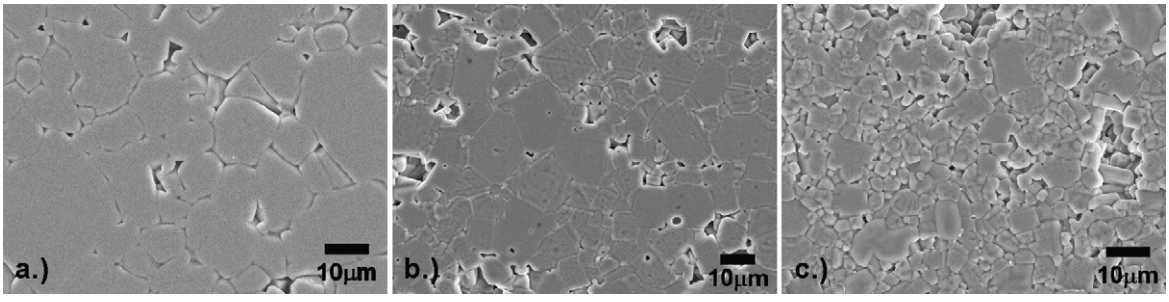

Fig. 2. SEM secondary electron images of matrix grains in samples with (a) 0 mol%, (b) 0.5 mol% and (c) 2 mol% $K_4CuNb_8O_{23}$ after annealing at 1100 °C for 10 h.

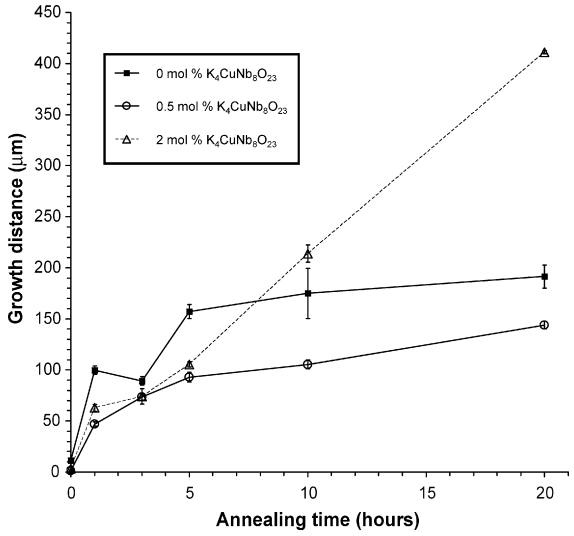

Fig. 3. Growth distance of single crystals vs. annealing time.

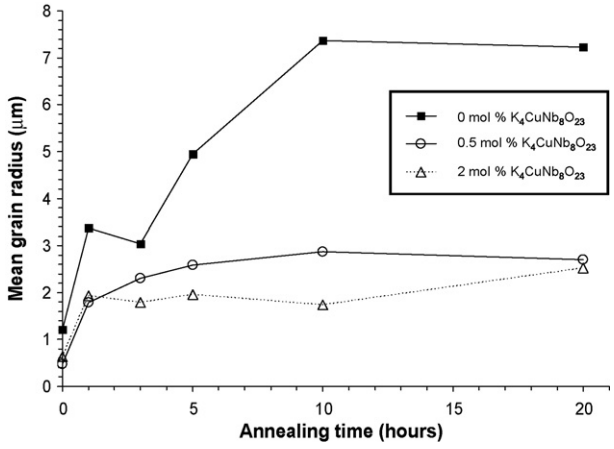

Fig. 4. Mean equivalent spherical 2D matrix grain size vs. annealing time.

The increase in mean grain size with annealing time is also less pronounced in these samples. Grain growth effectively ceases after 5 h at a mean grain radius of 2.5 μm. In the samples with 2 mol% $K_4CuNb_8O_{23}$, the matrix grains grow in the first hour, but then growth is stagnant until 10 h, the mean grain radius remaining constant at 2 μm. Between 10 and 20 h, the mean grain radius increases to 2.5 μm.

Table 1 gives the EDS analyses of the single crystals and matrix grains in samples annealed at 1100 °C for 10 h. Each value is the mean and standard deviation of eight point measurements. During point measurements, areas close to the Cu-containing second phases were avoided. Measurements are given for the A-site cations (i.e. K and Na) only: the value for the B-site cation (Nb) is assumed to be 20 at.%. ABO_3 stoichiometry was assumed. The measurement error for EDS is 5% relative to each mean value, i.e. ~0.5 at.%.[18] The nominal K and Na values for $(K_{0.5}Na_{0.5})NbO_3$ are also given. For the samples with 0 and 0.5 mol% $K_4CuNb_8O_{23}$, the composition of both the single crystal and the matrix grains is close to the nominal composition for $(K_{0.5}Na_{0.5})NbO_3$. For the sample with 2 mol% $K_4CuNb_8O_{23}$, the single crystal is Na-rich. However, the composition of the matrix grains is close to the nominal composition. Measurements were also carried out on crystals in samples with 2 mol% $K_4CuNb_8O_{23}$ annealed for 1 and 20 h, with similar results. The variation in composition of all the single crystals is <1 at.%, indicating that they are chemically homogenous.

4. Discussion

4.1. Solid-state single crystal growth

Addition of 0.5 and 2 mol% $K_4CuNb_8O_{23}$ caused a decrease in the growth rate of the single crystals. However, this behaviour is then reversed at annealing times >5 h for the samples containing 2 mol% $K_4CuNb_8O_{23}$, which display more crystal growth than the samples with 0 and 0.5 mol% $K_4CuNb_8O_{23}$. In order to explain this behaviour, the structure of the boundaries and the effect of the liquid phase on single crystal and matrix grain growth during annealing must be considered, as the growth behaviour of the single crystal is controlled by both these factors.

Ceramics have two types of boundaries: atomically rough and atomically faceted. Atoms can attach to any point on the surface of a grain with an atomically rough boundary and the growth rate of the grain increases linearly with the driving force for grain growth. $(K_{0.5}Na_{0.5})NbO_3$ has faceted grain boundaries (Fig. 2, also see Birol et al.[3] and Jenko et al.[17]). In ceramics with faceted boundaries, the attachment of atoms to the grain is energetically unfavourable. Atoms can only attach to the grain if a favourable site, such as a ledge, 2D nucleus or screw dislocation is present.[19,20] As a result, the growth rate of the grain does not increase linearly with the driving force for grain growth. In the case of 2D nucleation-controlled growth, the growth rate is given by

$$\dot{R} = \nu_{st} \exp\left(\frac{-\Delta G^*}{3kT}\right) \quad (1)$$

Table 1
EDS analyses of single crystals and matrix grains of samples annealed at 1100 °C for 10 h

Amount of $K_4CuNb_8O_{23}$ (mol%)	K (at.%)	Na (at.%)	K/Na ratio
0 (single crystal)	10.34 ± 0.58	10.82 ± 0.64	0.96 ± 0.04
0 (matrix)	10.64 ± 0.62	10.53 ± 0.58	1.01 ± 0.05
0.5 (single crystal)	10.41 ± 0.44	10.39 ± 0.41	0.99 ± 0.05
0.5 (matrix)	10.48 ± 0.63	10.42 ± 0.96	1.02 ± 0.13
2 (single crystal)	8.46 ± 0.54	13.35 ± 0.65	0.64 ± 0.06
2 (matrix)	10.58 ± 0.32	10.79 ± 0.99	0.99 ± 0.10
Nominal composition for $(K_{0.5}Na_{0.5})NbO_3$	10	10	1

where v_{st} is the step velocity of the growing 2D nucleus and ΔG^* is the free energy barrier for the formation of stable 2D nuclei. ΔG^* is given by

$$\Delta G^* = \frac{\pi \Omega \varepsilon^2}{2h\Delta\mu} \quad (2)$$

where Ω is the molar volume, ε the edge free energy of the 2D nucleus, h the step height of the nucleus and $\Delta\mu$ is the driving force for grain growth. ΔG^* is inversely proportional to the driving force $\Delta\mu$. Growth is effectively negligible below a critical driving force $\Delta\mu_C$ because very few stable 2D nuclei form. Most of the atoms adsorbing onto the grain surface are unable to reach a 2D nucleus before desorbing again. Above the critical driving force, stable 2D nuclei can form and the grain growth rate increases exponentially with driving force. Above $\Delta\mu_C$, kinetic roughening occurs—so many 2D nuclei form that any atom that adsorbs onto the surface of the grain can reach a 2D nucleus and attach to it. The boundary now behaves like an atomically rough boundary and the growth rate increases linearly with driving force. The single crystal will behave in the same way as the matrix grains, as it is essentially just a very large grain. This type of dependency of the growth rate on driving force has been measured for single crystals of alumina grown by solid-state crystal growth using a calcium aluminosilicate liquid phase.[21]

The driving force for grain growth is given by[22,23]

$$\Delta\mu = \sigma\Omega\left(\frac{1}{\bar{r}} - \frac{1}{r}\right) \quad (3)$$

where σ is the average interfacial energy (grain boundary energy or solid/liquid interfacial energy), r the radius of the growing grain and $\bar{r}$ is the mean grain radius. The radius of the growing single crystal is much larger than that of the matrix grains and so Eq. (3) can be approximated to

$$\Delta\mu = \frac{\sigma\Omega}{\bar{r}} \quad (4)$$

For single crystals or matrix grains with a driving force $>\Delta\mu_C$, growth is controlled by the rate at which atoms can diffuse across the boundaries. Addition of a small amount of liquid phase can increase the diffusion rate and the growth rate.[24] The increased diffusion rate offsets the increase in the boundary thickness. As more liquid phase is added the thickness of the liquid film at the boundaries increases, increasing the diffusion distance and lowering the growth rate.

Comparison of Figs. 3 and 4 shows a good correlation between the single crystal growth and matrix grain growth. In the samples with 0 mol% $K_4CuNb_8O_{23}$, the crystal growth rate is initially rapid, then tails off and becomes very low at annealing times above 5 h. Matrix grain growth is also initially rapid, but then slows down after 5 h, becoming stagnant after 10 h. In the samples with 0.5 mol% $K_4CuNb_8O_{23}$, both crystal and matrix grain growth are also initially rapid but tail off with annealing time, becoming almost constant after 5 h. Combining Eqs. (4), (2) and (1) shows that the single crystal growth rate decreases exponentially as the mean matrix grain size increases. At short annealing times, the matrix grain size is small and therefore the driving force for crystal growth and the growth rate are high. As the matrix grains grow the driving force for single crystal growth is reduced and the crystal growth rate slows. Finally, when matrix grain growth stops the driving force for crystal growth and hence the growth rate becomes constant. If the driving force drops below $\Delta\mu_C$, the growth rate will decrease exponentially. This can be seen in Fig. 3, where the growth rate for the samples with 0 and 0.5 mol% $K_4CuNb_8O_{23}$ becomes very low after 5 h.

In the samples with 2 mol% $K_4CuNb_8O_{23}$, matrix grain growth is rapid in the first hour but then is stagnant for annealing times up to 10 h. Likewise, the single crystal growth rate is high in the first hour but then becomes almost constant after 3 h. The constant matrix grain size causes the driving force and the single crystal growth rate to remain constant. After 10 h, the matrix grains begin to grow slowly. This causes a small reduction in driving force and single crystal growth begins to slow down. When compared with the other samples, the growth rate of the samples with 2 mol% $K_4CuNb_8O_{23}$ remains quite high up to an annealing time of 20 h. The driving force for growth appears to remain above $\Delta\mu_C$ throughout annealing.

The effect of addition of the liquid phase will now be considered. Addition of 0.5 mol% $K_4CuNb_8O_{23}$ causes growth of the single crystal to be slower than in the samples with 0 mol% $K_4CuNb_8O_{23}$ (Fig. 3) and also reduces growth of the matrix grains (Fig. 4). $(K_{0.5}Na_{0.5})NbO_3$ sintered without addition of a liquid phase sintering aid has boundaries with no liquid phase present.[17] When $K_4CuNb_8O_{23}$ is added, a liquid phase forms during sintering at 1100 °C which penetrates the boundaries and wets the grains.[25,26] It appears that the liquid film between the single crystal and the matrix grains is already thick enough to cancel out any increase in diffusion rate caused by the liquid and also any increase in driving force caused by the smaller matrix grain size. With addition of 2 mol% $K_4CuNb_8O_{23}$, the thickness of the liquid film between grains increases and matrix grain growth becomes stagnant or very slow, although single crystal growth is not affected. Because matrix grain growth is stagnant or very slow in these samples, the driving force for single crystal growth remains almost constant up to an annealing time of 20 h. Although the single crystal growth rate is initially lower for the samples with 2 mol% $K_4CuNb_8O_{23}$ than for the other samples, it remains almost constant during annealing, whereas the growth rate for the other samples drops rapidly after 5 h. This allows the single crystals in the samples with 2 mol% $K_4CuNb_8O_{23}$ to keep growing and eventually overtake the single crystals in the samples with 0 and 0.5 mol% $K_4CuNb_8O_{23}$. By an annealing time of 20 h, matrix grain growth has started to take place in the samples with 2 mol% $K_4CuNb_8O_{23}$. This will eventually cause the driving force for single crystal growth to decrease to a value below the critical driving force and single crystal growth should become very slow, as in the case of the samples with 0 and 0.5 mol% $K_4CuNb_8O_{23}$.

The effect that addition of a liquid has on the growth of single crystals of $(K_{0.5}Na_{0.5})NbO_3$ is different to that of a liquid on growth of single crystals of PMN-PT. Addition of PbO up to a certain amount caused a liquid film to form at the boundaries, increasing the diffusion rate and causing an increase in both the

single crystal and matrix grain growth rates. Further additions of PbO either caused a decrease in growth rate[14] or had no effect,[15] depending on whether growth was diffusion or interface reaction controlled. In the present study, addition of as little as 0.5 mol% of $K_4CuNb_8O_{23}$ liquid phase is enough to reduce the growth rate of the single crystal and the matrix grains. This is possible if the liquid films at the boundaries are thick enough to cancel out the increase in diffusion rate caused by the liquid. The reduction in the matrix grain size will increase the driving force for single crystal growth in the samples with 0.5 mol% $K_4CuNb_8O_{23}$, which should lead to an increase in growth rate. However, this is counteracted by the increase in thickness of the liquid film between the single crystal and the matrix grains, leading to a reduction in the growth rate of the single crystals. The liquid film between the single crystal and the matrix grains is likely to be relatively thick due to the accumulation of liquid phase at the boundary during crystal growth. Addition of 2 mol% liquid phase reduces the growth rate of the matrix grains further by increasing the thickness of the liquid films, implying that grain growth is controlled by diffusion through the liquid film. This is expected, as grains with a driving force higher than $\Delta\mu_C$ undergo kinetic roughening and grain growth is then controlled by diffusion. Single crystal growth is not slowed down further by the increase in liquid phase from 0.5 to 2 mol%. This may be due to the increase in driving force caused by the smaller matrix grain size. There may also be a limiting value to the film thickness at the single crystal/matrix boundary, with excess $K_4CuNb_8O_{23}$ being incorporated in the single crystal (Fig. 1(d)).

4.2. Chemical composition of the single crystals

The EDS results show that single crystals grown in samples with 0 and 0.5 mol% $K_4CuNb_8O_{23}$ have compositions close to the expected $(K_{0.5}Na_{0.5})NbO_3$ composition and are chemically homogenous (Table 1). However, single crystals grown in the samples with 2 mol% $K_4CuNb_8O_{23}$ are Na-rich, while the matrix grains are of $(K_{0.5}Na_{0.5})NbO_3$ composition (Table 1). This change in composition can be explained by considering the effect of addition of $K_4CuNb_8O_{23}$ on the phase equilibria of the system. According to the $KNbO_3$–$NaNbO_3$ pseudo-binary phase diagram, at 1100 °C $(K_{0.5}Na_{0.5})NbO_3$ lies just below the solidus line and is the equilibrium phase.[1] Addition of $K_4CuNb_8O_{23}$ changes the system from a two-component into a three-component system. No phase diagram exists for this system, but because the amount of $K_4CuNb_8O_{23}$ added is quite low we can use the $KNbO_3$–$NaNbO_3$ pseudo-binary phase diagram as a guide to what will happen. $KNbO_3$ has a melting point of 1058 °C.[27] $NaNbO_3$ has a melting point of 1242 °C.[28] The melting point of $K_4CuNb_8O_{23}$ is 1050 °C.[26] The melting point of $K_4CuNb_8O_{23}$ is lower than that of $KNbO_3$ and $NaNbO_3$, therefore addition of $K_4CuNb_8O_{23}$ will lower the solidus temperature. Addition of 2 mol% $K_4CuNb_8O_{23}$ may be enough to lower the solidus temperature so that the samples are now in a liquid + solid two-phase field at 1100 °C. From the pseudo-binary phase diagram, it can be seen that the equilibrium solid phase will be richer in Na than in K. Therefore the growing single crystal should be Na-rich, as is the case. The matrix grains should remain at the $(K_{0.5}Na_{0.5})NbO_3$ composition as grain growth is very slow.

One of the advantages of the SSCG method is that the crystals have the same composition as the matrix powder, which simplifies the growth of materials which melt incongruently.[29] The EDS results in Table 1 show that this is the case for single crystals of $(K_{0.5}Na_{0.5})NbO_3$ grown by SSCG from samples with 0 or 0.5 mol% $K_4CuNb_8O_{23}$. However, the crystals grown from samples with 2 mol% $K_4CuNb_8O_{23}$ were not of the expected composition, due to the lowering of the solidus temperature. To our knowledge, this is the first time that such an effect has been reported in single crystals grown by SSCG. Care may have to be taken when adding a liquid phase sintering aid to systems where crystal growth takes place at temperatures close to the solidus temperature. The crystals grown in samples with 2 mol% $K_4CuNb_8O_{23}$ also have Cu-containing inclusions trapped within them. Entrapment of the liquid phase was also noticed during growth of PMN-PT single crystals.[14,15] The presence of inclusions is likely to be detrimental to the piezoelectrical properties of the crystal.

5. Conclusions

The effect of addition of $K_4CuNb_8O_{23}$ liquid phase sintering aid on the growth of single crystals of $(K_{0.5}Na_{0.5})NbO_3$ by the solid-state crystal growth method has been studied. The results show that the single crystal growth rate can be retarded or enhanced by the addition of $K_4CuNb_8O_{23}$ liquid phase sintering aid. Addition of 0.5 mol% $K_4CuNb_8O_{23}$ caused a reduction in the single crystal and matrix grain growth rates compared to that of samples with 0 mol% $K_4CuNb_8O_{23}$. This was due to the increased diffusion distance across the boundaries caused by liquid films at the boundaries. Addition of 2 mol% $K_4CuNb_8O_{23}$ further reduced the matrix grain growth rate. Single crystal growth in the samples with 0 and 0.5 mol% $K_4CuNb_8O_{23}$ was initially rapid and then tailed off with annealing time. This was due to a reduction in driving force for single crystal growth caused by grain growth in the matrix. In the samples with 2 mol% $K_4CuNb_8O_{23}$, the driving force for single crystal growth remained almost constant due to stagnant or very slow grain growth in the matrix. The crystal growth rate remained almost constant with annealing time and at longer annealing times the growth distance of the single crystals was greater than that of the other samples. The single crystals grown from powders with 0 and 0.5 mol% $K_4CuNb_8O_{23}$ had compositions close to the expected $(K_{0.5}Na_{0.5})NbO_3$ composition. However, the single crystals grown from powder with 2 mol% $K_4CuNb_8O_{23}$ were Na-rich. This was due to lowering of the solidus temperature by $K_4CuNb_8O_{23}$.

Acknowledgements

This project was supported by the European Union under the Sixth Framework project IMMEDIATE and by the National project Electronic Ceramics, Nano, 2D in 3D Structures. The authors would like to thank D. Rytz and S. Vernay (FEE GmbH) for providing the $KTaO_3$ seed crystals. The authors would also

like to thank J. Cilenšek and S. Drnovšek for technical support and T. Kenda for assistance with preparation of the powder.

References

1. Jaffe, B., Cook Jr., W. R. and Jaffe, H., *Piezoelectric Ceramics*. Academic Press, London, 1971, pp. 192–193.
2. Zhang, B. P., Li, J. F., Wang, K. and Zhang, H., Compositional dependence of piezoelectric properties in $Na_xK_{1-x}NbO_3$ lead-free ceramics prepared by spark plasma sintering. *J. Am. Ceram. Soc.*, 2006, **89**(5), 1605–1609.
3. Birol, H., Damjanovic, D. and Setter, N., Preparation and characterization of $(K_{0.5}Na_{0.5})NbO_3$ ceramics. *J. Eur. Ceram. Soc.*, 2004, **26**, 861–866.
4. Hollenstein, E., Davies, M., Damjanovic, D. and Setter, N., Piezoelectric properties of Li- and Ta-modified $(K_{0.5}Na_{0.5})NbO_3$ ceramics. *Appl. Phys. Lett.*, 2005, **87**, 182905-1–182905-3.
5. Saito, Y., Takao, H., Tani, T., Nonoyama, T., Takatori, K., Homma, T., Nagaya, T. and Nakamura, M., Lead-free piezoceramics. *Nature*, 2004, **432**, 84–87.
6. Sheets, S. A., Soukhojak, A. N., Ohasi, N. and Chiang, Y. M., Relaxor single crystals in the $(Bi_{1/2}Na_{1/2})_{1-x}Ba_xZr_yTi_{1-y}O_3$ system exhibiting high electrostrictive strain. *J. Appl. Phys.*, 2001, **90**(10), 5287–5295.
7. Wada, S., Muraoka, K., Kakemoto, H., Tsurumi, T. and Kumagai, H., Enhanced piezoelectric properties of potassium niobate single crystals by domain engineering. *Jpn. J. Appl. Phys.*, 2004, **43**(9B), 6692–6700.
8. Shirane, G., Newnham, R. and Pepinsky, R., Dielectric properties and phase transitions of $NaNbO_3$ and (Na, K)NbO_3. *Phys. Rev.*, 1954, **96**(1), 581–588.
9. Ahtee, M. and Glazer, A. M., Lattice parameters and tilted octahedra in sodium–potassium niobate solid solutions. *Acta Cryst. A*, 1976, **32**, 434–446.
10. Raevskiĭ, I. P., Reznichenko, L. A., Ivliev, M. P., Smotrakov, V. G., Eremkin, V. V., Malitskaya, M. A., Shilkina, L. A., Shevtsova, S. I. and Borodin, A. V., Growth and study of single crystals of (Na, K)NbO_3 solid solutions. *Crystall. Rep.*, 2003, **48**(3), 486–490.
11. Kizaki, Y., Noguchi, Y. and Miyayama, M., Defect control for superior properties in $K_{0.5}Na_{0.5}NbO_3$ single crystals. *Key Eng. Mater.*, 2007, **350**, 85–88.
12. Fisher, J. G., Benčan, A., Holc, J., Kosec, M., Vernay, S. and Rytz, D., Growth of potassium sodium niobate single crystals by solid state crystal growth. *J. Crystal Growth*, 2007, **303**(2), 487–492.
13. Fisher, J. G., Benčan, A., Bernard, J., Holc, J., Kosec, M., Vernay, S. and Rytz, D., Growth of (Na, K, Li)(Nb, Ta)O_3 single crystals by solid state crystal growth. *J. Eur. Ceram. Soc.*, 2007, **27**, 4103–4106.
14. King, P. T., Gorzkowski, E. P., Scotch, A. M., Rockosi, D. J., Chan, H. M. and Harmer, M. P., Kinetics of {0 0 1} $Pb(Mg_{1/3}Nb_{2/3})O_3$–35 mol% $PbTiO_3$ single crystals grown by seeded polycrystal conversion. *J. Am. Ceram. Soc.*, 2003, **86**(12), 2182–2187.
15. Gorzkowski, E. P., Chan, H. M. and Harmer, M. P., Effect of PbO on the kinetics of {0 0 1} $Pb(Mg_{1/3}Nb_{2/3})O_3$–35 mol% $PbTiO_3$ single crystals grown into fully dense matrices. *J. Am. Ceram. Soc.*, 2006, **89**(3), 856–862.
16. Samardžija, Z., Bernik, S., Marinenko, R. B., Malič, B. and Čeh, M., An EPMA study on $KNbO_3$ and $NaNbO_3$ single crystals—potential reference materials for quantitative microanalysis. *Microchim. Acta*, 2004, **145**, 203–208.
17. Jenko, D., Benčan, A., Malič, B., Holc, J. and Kosec, M., Electron microscopy studies of potassium sodium niobate ceramics. *Microsc. Microanal.*, 2005, **11**, 572–580.
18. Goldstein, J., Newbury, D., Joy, D., Lyman, C., Echlin, P., Lifshin, E., Sawyer, L. and Michael, J., *Scanning Electron Microscopy and X-ray Microanalysis* (*3rd ed.*). Kluwer Academic/Plenum Publisher, New York, 2003, p. 421.
19. Hirth, J. P. and Pound, G. M., *Condensation and Evaporation: Nucleation and Growth Kinetics*. Pergamon Press, Oxford, 1963, pp. 77–106.
20. Van der Eerden, J. P., Crystal growth mechanisms. In *Handbook of Crystal Growth, vol. 1: Fundamentals, Part A, Thermodynamics and Kinetics*, ed. D. T. J. Hurle. Elsevier Science Publishers, Amsterdam, The Netherlands, 1993, pp. 311–475.
21. Seabaugh, M. M., Suvaci, E., Brahmaroutu, B. and Messing, G. L., Modeling anisotropic single crystal growth kinetics in liquid phase sintered α-Al_2O_3. *Interf. Sci.*, 2000, **8**, 257–267.
22. Park, Y. J., Hwang, N. M. and Yoon, D. Y., Abnormal growth of faceted (WC) grains in a (Co) liquid matrix. *Metall. Mater. Trans. A*, 1996, **27**, 2809–2819.
23. Yoon, D. Y., Park, C. W. and Koo, J. B., The step growth hypothesis for abnormal grain growth. In *Interfaces*, *vol. 2*, ed. H. I. Yoo and S.-J. L. Kang. Institute of Materials, London, 2001. p. 12.
24. Powers, J. D. and Glaeser, A. M., Grain boundary migration in ceramics. *Interf. Sci.*, 1998, **6**, 23–29.
25. Matsubara, M., Yamaguchi, T., Sakamoto, W., Kikuta, K., Yogo, T. and Hirano, S. I., Processing and piezoelectric properties of lead-free (K, Na)(Nb, Ta)O_3 ceramics. *J. Am. Ceram. Soc.*, 2005, **88**(5), 1190–1196.
26. Matsubara, M., Yamaguchi, T., Kikuta, K. and Hirano, S., Sinterability and piezoelectric properties of (K, Na)NbO_3 ceramics with novel sintering aid. *Jpn. J. Appl. Phys.*, 2004, **43**(10), 7159–7163.
27. Irle, E., Blachnik, R. and Gather, B., The phase diagrams of Na_2O and K_2O with Nb_2O_5 and the ternary system Nb_2O_5–Na_2O–Yb_2O_3. *Thermochim. Acta*, 1991, **179**, 157–169.
28. Roth, R. S., Parker, H. S., Brower, W. S. and Minor, D. B., Alkali oxide–tantalum oxide and alkali oxide–niobium oxide ionic conductors. *NASA Contract Rep. CR, Contract No. NASA-CR-134599*, 1974, pp. 1–59.
29. Lee, H. Y., Solid-state single crystal growth (SSCG) method: a cost-effective way of growing piezoelectric single crystals. In *Piezoelectric Single Crystals*, ed. S. Trolier-McKinstry, L. E. Cross and Y. Yamashita. S. Trolier-McKinstry, 2004, pp. 160–177.